

High-spin states in ^{107}In and ^{108}In

E. Andersson, P. Herges, H. V. Klapdor, and I. N. Wischnewski*

Max-Planck-Institut für Kernphysik, Heidelberg, Germany

(Received 13 April 1981)

High-spin states in $^{107,108}\text{In}$ have been investigated using the $^{92}\text{Mo}(^{19}\text{F}, 2pxn\gamma)^{107,108}\text{In}$ reaction. In-beam measurements of γ - γ coincidences, γ -ray excitation functions, and γ -ray angular distributions were performed with Ge(Li) detectors, one of which had a NaI Compton suppression shield. Level schemes for ^{107}In and ^{108}In have been constructed up to states with $I^\pi = (29/2^-)$ and (16^-) , respectively.

NUCLEAR REACTIONS $^{92}\text{Mo}(^{19}\text{F}, 2pxn\gamma)^{107,108}\text{In}$, $E = 65 - 105$ MeV; measured E_γ , γ - γ coincidences, γ -ray angular distributions. $^{107,108}\text{In}$ deduced high-spin states. Enriched target. Anti-Compton spectrometer.

I. INTRODUCTION

The indium isotopes have one proton hole in the $Z = 50$ shell. From transfer reactions^{1,2} the three lowest lying states in the odd In nuclei are well established as $g_{9/2}$, $p_{1/2}$, and $p_{3/2}$ proton-hole states. The structure of the corresponding core nuclei, the Sn isotopes, has been described by neutron quasiparticle excitations (e.g., Ref. 3). In the region around $Z = 50$ data also exist supporting an interpretation of the observed level schemes in terms of a small deformation. Low-lying low-spin positive parity states in the odd indium isotopes have been suggested^{4,5} to be members of a rotational band associated with the Nilsson orbital $\frac{1}{2}^+[431]$. In the even $^{112-118}\text{Sn}$ nuclei the observation of a quasirotational band has been reported,⁶ where the band head is supposed to be the first excited 0^+ state. Potential energy calculations for odd In (Ref. 5) and even Sn (Ref. 7) nuclei have actually given a minimum for the band heads in question at a moderate prolate deformation ($\epsilon \cong 0.2$ and 0.1 , respectively). The even Cd ($Z = 48$) isotopes are known to exhibit rotational characteristics^{8,9} due to a small deformation.

In the odd $^{113,115}\text{In}$ nuclei multiplets of states have been found,^{10,11} arising from the coupling of a $g_{9/2}$ proton hole to a quadrupole phonon of the even Sn core. High-spin states in ^{109}In (Ref. 12) and ^{111}In (Ref. 13) have also been interpreted within a hole-core coupling model.

In a recent study¹⁴ of high-spin states in ^{108}In a rotor + two quasiparticle model has been suggested for the lower band. Level sequences of negative

parity states between 3^- and 10^- observed in the odd-odd $^{110-114}\text{In}$ nuclei were explained by the $(\pi g_{9/2})^{-1}(\nu h_{11/2})$ configuration considering a two- and three-parameter effective neutron-proton interaction.¹⁵ Reference 16 investigates how the coupling mode in the odd-odd nuclei may be influenced by the positions of the Fermi surfaces and the deformations β and γ .

In this situation it seemed interesting to extend the existing high-spin investigations to the neutron-deficient region at $Z \cong 50$. This is done in this paper by studying high-spin states in ^{107}In and ^{108}In . Particularly for the ^{107}In nucleus the previous information on high-spin states was very scarce.

The present γ spectroscopic study is part of a program, extending recent studies of yrast lines in light nuclei,¹⁷⁻²⁰ for investigating high-spin states in nuclei near closed shells, where coexistence of single particle and collective behavior is expected. In the course of this program we have recently investigated yrast lines near the closed shells $Z = 20$, $N = 20$ ($^{34,37}\text{Cl}$, ^{40}K , ^{42}Ca),^{21,22} $Z = 28$, $N = 28$ ($^{55,56}\text{Fe}$),²³ and $Z = 50$ (^{108}Sn , ^{106}In),^{24,25} and the β^+ decay of high-spin isomers in $^{105,106,108}\text{In}$ and $^{100,102}\text{Ag}$.²⁶

II. EXPERIMENTAL PROCEDURE AND RESULTS

The experiments were performed at the Emperor Tandem at the Max-Planck-Institut in Heidelberg. Excitation functions, angular distributions, and γ - γ coincidences were measured for γ transitions in ^{107}In and ^{108}In produced in the

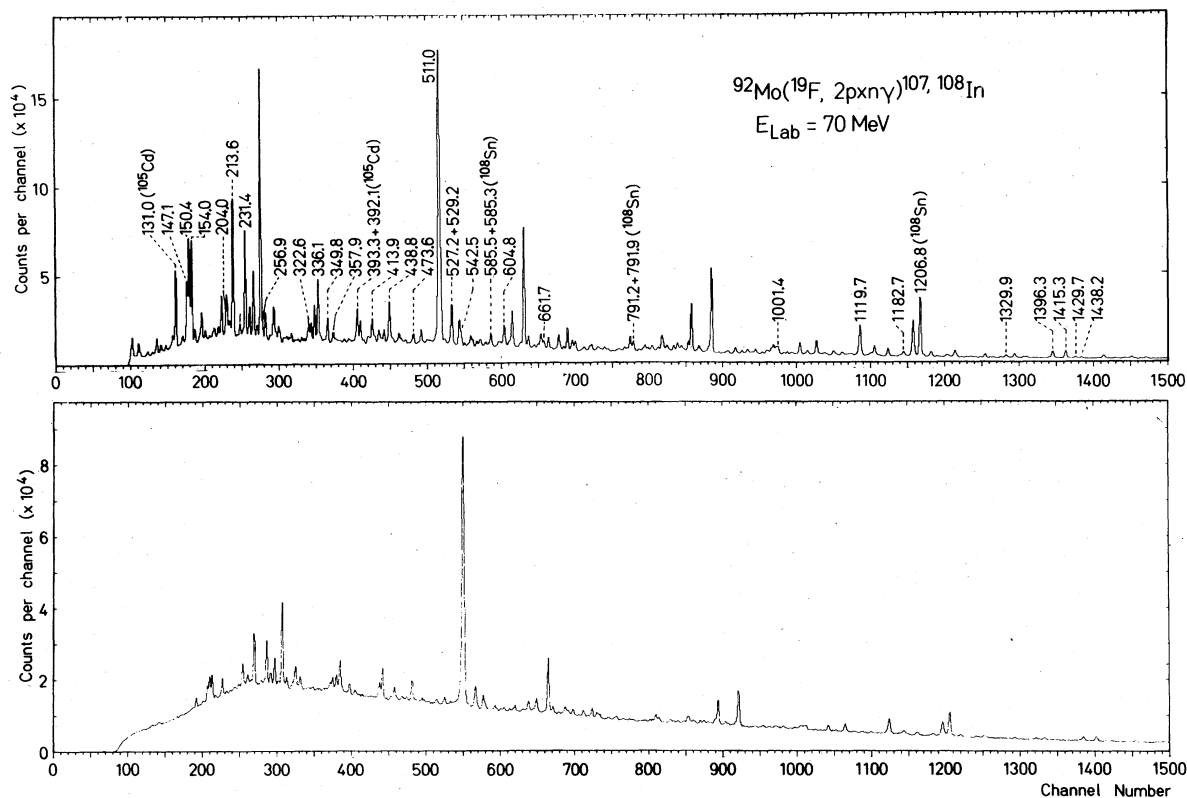


FIG. 1. Total projection γ - γ coincidence spectra of the reaction $^{92}\text{Mo}(^{19}\text{F},xyz)$ measured at $E_{\text{lab}} = 70 \text{ MeV}$. The upper part shows the spectrum taken with the anti-Compton spectrometer; in the lower part the corresponding spectrum of the unshielded Ge(Li) detector is displayed. Energies are given for the lines attributed to ^{107}In and ^{108}In and for the ground state transitions of ^{105}Cd and ^{108}Sn , respectively.

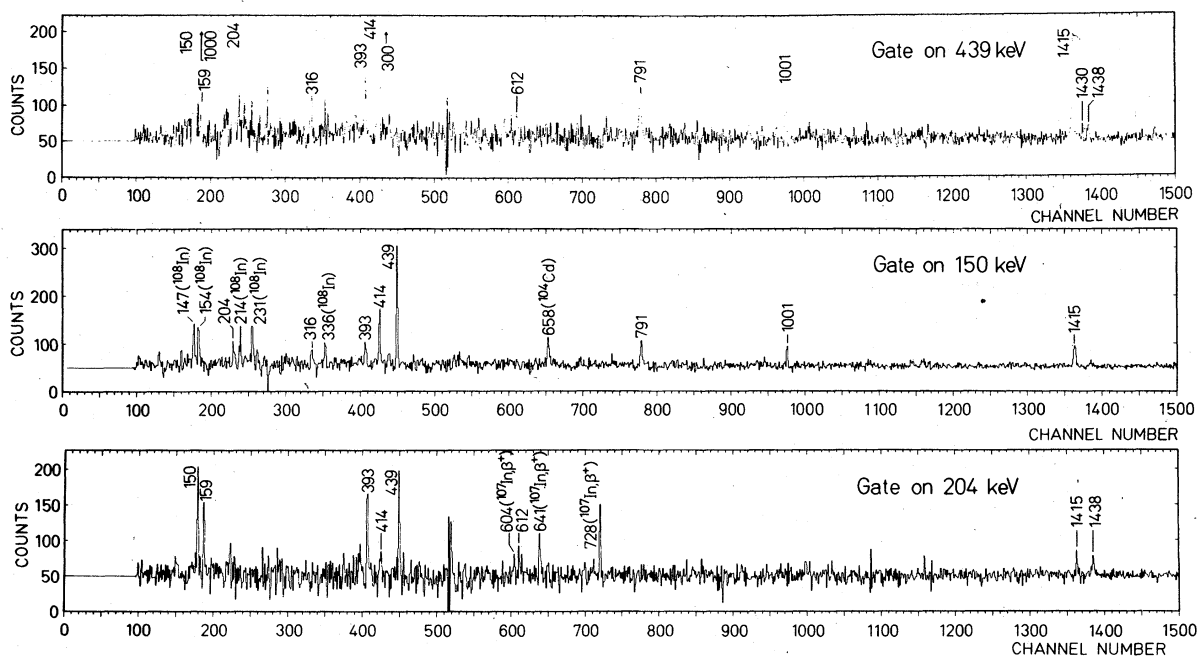


FIG. 2. Examples of γ - γ coincidence spectra (background subtracted) from the $^{92}\text{Mo}(^{19}\text{F}, 2p 2n)^{107}\text{In}$ reaction at 70 MeV. An arbitrary number of 50 is added to the intensity.

$^{92}\text{Mo}(^{19}\text{F},xyz)$ reaction. The Mo target enriched to 98% in ^{92}Mo consisted of a 2 mg/cm² thick Mo layer sputtered onto a Pb backing of ~ 50 mg/cm².

In the γ - γ coincidence measurements two Ge(Li) detectors were used with efficiencies of 26%. The energy resolution was typically 2.3 keV at 1332 keV. One of the Ge(Li) detectors was equipped with a NaI(Tl) Compton suppression shield giving a Compton background suppression factor of better than 8:1 (see Fig. 1 and Ref. 27). From statistical model calculations with the computer code CAS-

CADE (written by Pühlhofer²⁸) the appropriate ^{19}F beam energy was chosen to be 70 MeV,²⁴ to enable a simultaneous study of $^{107,108}\text{In}$ and ^{108}Sn . In Fig. 1 the total projections of the coincidence spectrum are displayed. The Ge(Li) detectors were placed at $\pm 90^\circ$ with respect to the beam axis. The γ - γ - Δt events were stored on magnetic tape with a PDP 11/45 computer, and further analysis was done with a DEC 10 computer. The coincidence counting rate was kept at about 120 Hz and a total of 1.6×10^7 events were recorded. Examples of coin-

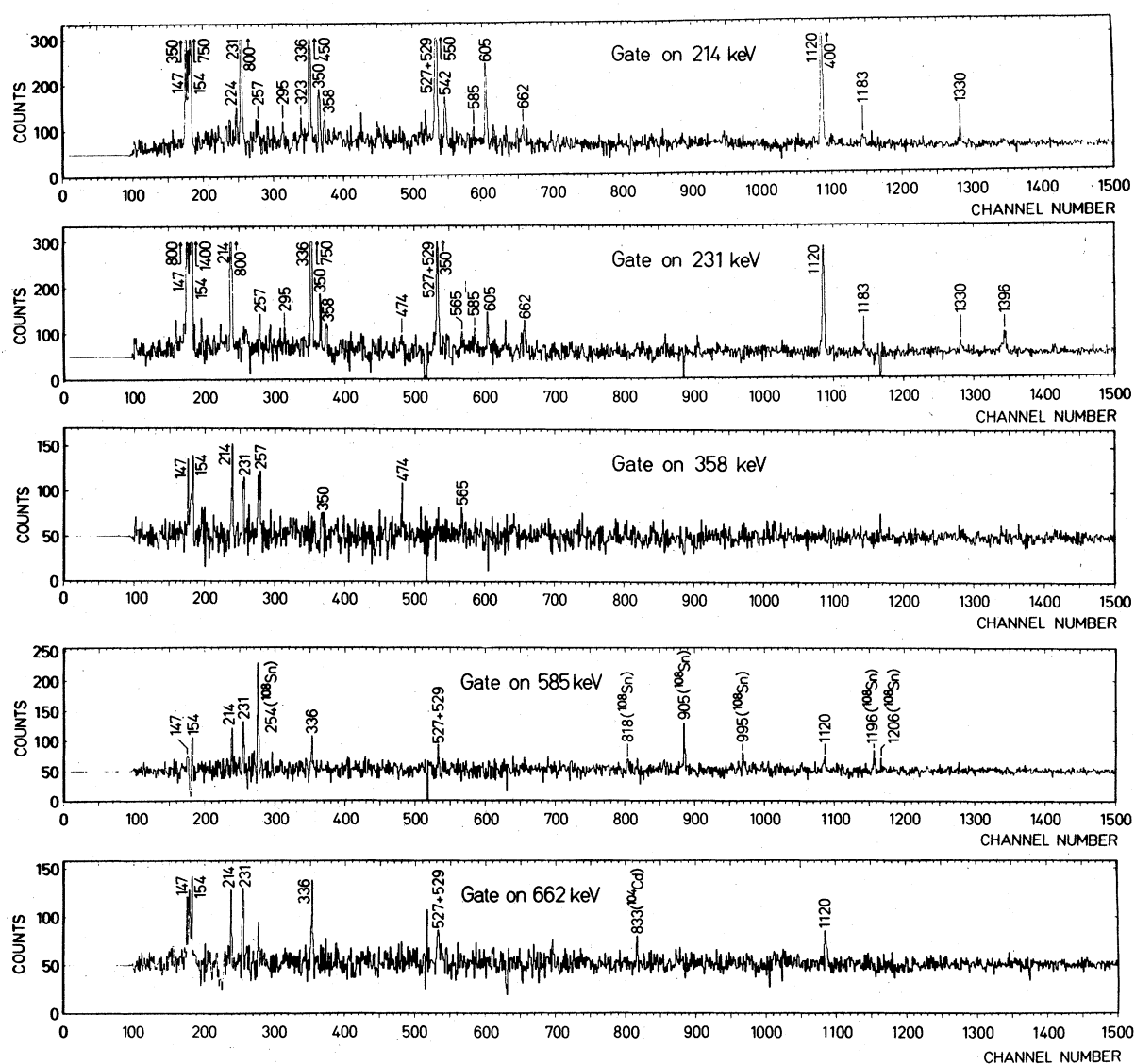


FIG. 3. Examples of γ - γ coincidence spectra (background subtracted) from the $^{92}\text{Mo}(^{19}\text{F},2pn)^{108}\text{In}$ reaction at 70 MeV. An arbitrary number of 50 is added to the intensity.

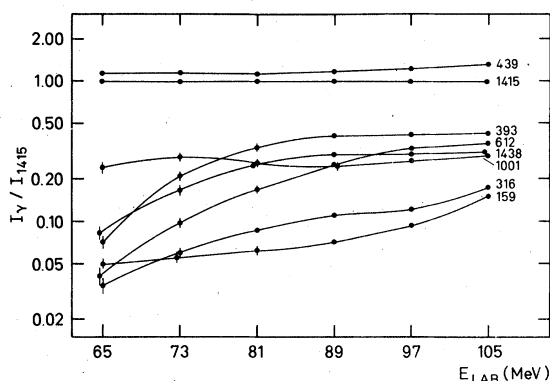


FIG. 4. Relative yields of some γ transitions in ^{107}In as a function of bombarding energy in the $^{92}\text{Mo}(^{19}\text{F}, 2p 2n\gamma)$ reaction. The intensities are normalized to that of the 1415 keV line.

cidence spectra corrected for accidental and background coincidences are shown in Figs. 2 and 3.

Singles γ -ray spectra were recorded with the anti-Compton spectrometer placed at 90° relative to the beam line for beam energies between 65 and 105 MeV varied in steps of 8 MeV. In Figs. 4 and 5 relative excitation functions of a number of γ transitions, corrected for angular distributions, are shown. For ^{108}In the total production yield at $E_{\text{lab}} = 105$ MeV was too low to allow an accurate analysis.

The angular distributions were measured at four angles (0° , 35° , 55° , and 90°) at $E_{\text{lab}} = 70$ MeV. The measurements were made with the anti-Compton

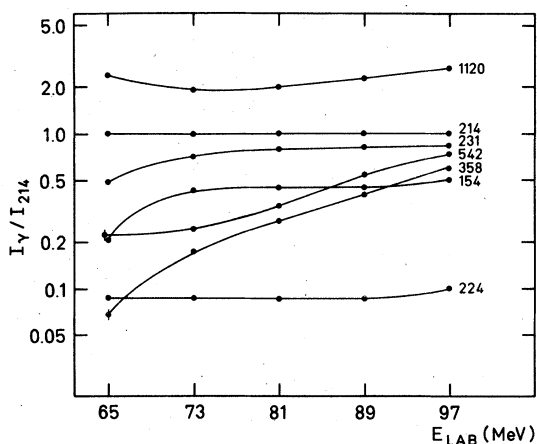


FIG. 5. Relative yields of some γ transitions in ^{108}In as a function of bombarding energy in the $^{92}\text{Mo}(^{19}\text{F}, 2pn\gamma)$ reaction. The intensities are normalized to that of the 214 keV line.

spectrometer, with a target-detector distance of 16 cm. The angular distribution of γ rays following a heavy ion reaction can be expressed with the relation

$$N(\theta) = N_0[1 + A_{22}P_2(\cos\theta) + A_{44}P_4(\cos\theta)].$$

The experimental data were compared to this function in a least-squares analysis, where the mixing ratio δ was changed in steps of 1° for $\arctan\delta$ between -90° and 90° . For the population of the magnetic substates a Gaussian distribution around $m = 0$ with a width σ was assumed. The values of σ were varied between $\sigma \cong 1.5 - 3.5$.

The analysis of the angular distributions was made on the basis of a 99.9% confidence limit. In cases of more than one possible solution, the one with the smallest $|\delta|$ was taken. Slight variations in σ did not change the results of the fits. The spin assignments were made assuming that high-spin states subsequently decay to states with lower spin. For small nonzero values of the mixing ratio δ the multipolarity of the given transition was assumed to be of mixed $M(\lambda)E(\lambda + 1)$ type. Examples of χ^2 fits are shown in Fig. 6. The results are summarized in Tables I and II.

III. THE LEVEL SCHEMES

A. ^{107}In

The proposed level scheme for ^{107}In is shown in Fig. 7. Very little was known before about high-spin states in ^{107}In . In a low-spin study of Dietrich *et al.*⁵ the three lowest transitions seen in this work below the 1415 keV level were observed. In a study of the even Sn isotopes²⁹ some of the strongest lines in ^{107}In were tentatively assigned to ^{107}Sn in view of excitation function results from the $^{106}\text{Cd} + \alpha$ reaction. However, the excitation curves for the (α, pxn) and $[\alpha, (x + 1)n]$ reactions are similar in this case, which our statistical model calculations for this reaction have also shown. Moreover, comparison of the total production cross section of ^{107}In in the $^{92}\text{Mo}(^{19}\text{F}, 2p 2n)^{107}\text{In}$ reaction as a function of the beam energy with CASCADE calculations indicates that the observed lines really belong to ^{107}In , as can be seen From Fig. 8.

The ground state has been established as a $\frac{9}{2}^+$ state,³⁰ similar to the ground states of the odd $^{109-119}\text{In}$ isotopes. The two low-lying $\frac{1}{2}^-$ and $\frac{3}{2}^-$ states known as $p_{1/2}$ and $p_{3/2}$ proton-hole states

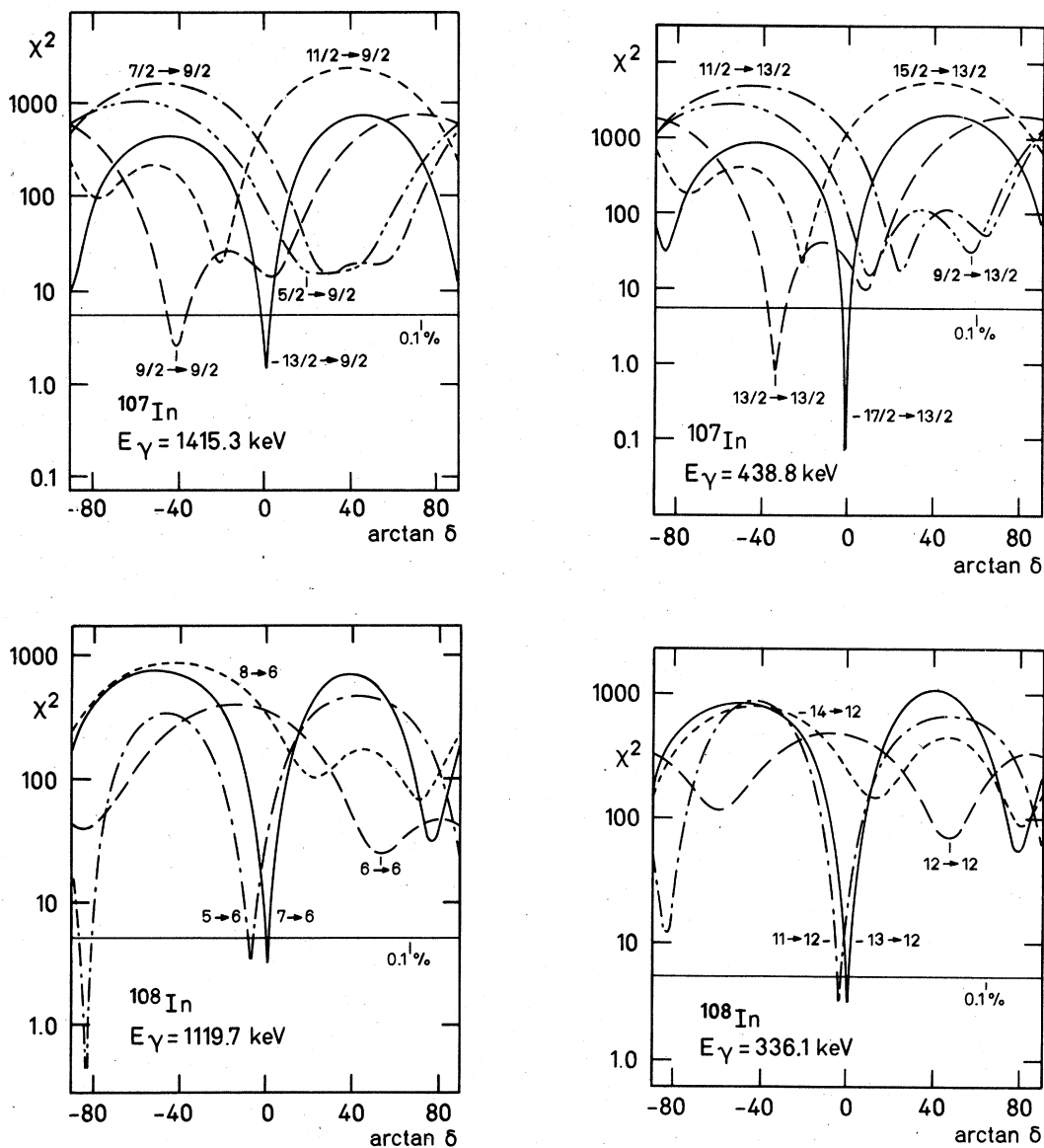


FIG. 6. Least-squares analysis of the angular distributions of some transitions in ^{107}In and ^{108}In , respectively.

could, because of the reaction mechanism, of course not be seen in this work.

The angular distribution coefficients of the 150, 439, and 1415 keV transitions are typical for $\Delta I = 2$ transitions, and a parity-conserving $E2$ assignment to these transitions is consistent with the mixing ratio values obtained. Levels with $I^\pi = \frac{11}{2}^+$ and $\frac{13}{2}^+$ have been observed in the odd $^{109-115}\text{In}$ nuclei¹⁰⁻¹³ at excitation energies similar to those in ^{107}In .

For the 791 keV transition no reliable angular distribution analysis could be performed, as it was strongly admixed by a transition of the same energy in ^{108}Sn .²⁴ It was not possible to resolve the 204 keV line from the very strongly seen 204.9 keV transition known from the β^+ decay of ^{107}In . This transition was assumed to be of $M1/E2$ multipolarity, which is consistent with the systematical behavior found in the neighboring In isotopes. Finally, proper corrections were made for admixtures

TABLE I. Energies (E_γ), intensities (I_γ), Legendre coefficients of angular distributions (A_{22}, A_{44}), deduced multipole mixing ratios (δ), minimum value of χ^2 fit, and corresponding spin-parity combination of initial and final state for the observed γ transitions in ^{107}In .

E_γ (keV)	I_γ	A_{22}	A_{44}	δ	χ^2_{red}	$J_i^\pi \rightarrow J_f^\pi$
150.4	61.3	0.41(3)	-0.16(3)	-0.01(4)	4.9	$\frac{21}{2}^+ \rightarrow \frac{17}{2}^+$
158.9	5.5	-0.13(4)	-0.05(4)	-0.06(7)	4.9	$\frac{23}{2}^- \rightarrow \frac{21}{2}^-$
				0.26(9)	5.2	$\frac{25}{2}^- \rightarrow \frac{21}{2}^-$
				0.97(24)	0.2	$\frac{21}{2}^- \rightarrow \frac{21}{2}^-$
				0.03(8)	4.9	$\frac{19}{2}^- \rightarrow \frac{21}{2}^-$
				-0.30(11)	0.4	$\frac{17}{2}^- \rightarrow \frac{21}{2}^-$
204.0	14.0 ^a	^b				
316.2	3.3	-0.11(3)	-0.03(3)	-0.06(3)	1.2	$\frac{23}{2}^+ \rightarrow \frac{21}{2}^+$
				0.03(3)	1.2	$\frac{19}{2}^- \rightarrow \frac{21}{2}^+$
				-0.31(7)	2.8	$\frac{17}{2}^- \rightarrow \frac{21}{2}^+$
393.3	11.9 ^c	-0.18(2)	0.04(2)	-0.04(2)	1.8	$\frac{27}{2}^- \rightarrow \frac{25}{2}^-$
				0.01(3)	1.7	$\frac{23}{2}^- \rightarrow \frac{25}{2}^-$
413.9	24.4 ^c	-0.04(1)	-0.00(1)	-0.13(3)	2.4	$\frac{13}{2}^+ \rightarrow \frac{11}{2}^+$
				0.07(3)	2.4	$\frac{9}{2}^+ \rightarrow \frac{11}{2}^+$
438.8	100	0.33(2)	-0.06(3)	-0.02(3)	0.05	$\frac{17}{2}^+ \rightarrow \frac{13}{2}^+$
				-0.69(9)	0.9	$\frac{13}{2}^- \rightarrow \frac{13}{2}^+$
611.8	3.5	-0.19(4)	0.13(4)	-0.07(4)	4.4	$\frac{29}{2}^- \rightarrow \frac{27}{2}^-$
				0.03(5)	4.4	$\frac{25}{2}^- \rightarrow \frac{27}{2}^-$
791.2	17.6 ^a	^b				
1001.4	27.2	0.01(2)	0.08(2)	-0.18(4)	4.0	$\frac{11}{2}^+ \rightarrow \frac{9}{2}^+$
				0.15(8)	4.7	$\frac{7}{2}^+ \rightarrow \frac{9}{2}^+$
1415.3	74.0	0.31(2)	-0.09(3)	0.01(3)	1.3	$\frac{13}{2}^+ \rightarrow \frac{9}{2}^+$
				-0.89(15)	2.5	$\frac{9}{2}^- \rightarrow \frac{9}{2}^+$
1429.7	11.7	0.16(5)	0.07(5)	0.03(15)	4.6	$\frac{21}{2}^- \rightarrow \frac{17}{2}^+$
				-0.28(9)	1.8	$\frac{19}{2}^+ \rightarrow \frac{17}{2}^+$
				0.35(22)	2.4	$\frac{17}{2}^- \rightarrow \frac{17}{2}^+$
				0.29(14)	1.9	$\frac{15}{2}^+ \rightarrow \frac{17}{2}^+$
				0.03(16)	2.1	$\frac{13}{2}^- \rightarrow \frac{17}{2}^+$
1438.2	8.3	-0.18(3)	-0.05(3)	0.00(4)	5.0	$\frac{23}{2}^- \rightarrow \frac{21}{2}^+$

TABLE I. (Continued).

E_γ (keV)	I_γ	A_{22}	A_{44}	δ	χ^2_{red}	$J_i^\pi \rightarrow J_f^\pi$
				-0.03(7)	5.0	$\frac{19}{2}^- \rightarrow \frac{21}{2}^+$
				-0.39(12)	3.7	$\frac{17}{2}^- \rightarrow \frac{21}{2}^+$

^aIntensity deduced from coincidence intensities.

^bNo coefficients given because the lines are strongly contaminated.

^cIntensity corrected for admixed line (see text).

TABLE II. Energies (E_γ), intensities (I_γ), Legendre coefficients of angular distributions (A_{22}, A_{44}), deduced multipole mixing ratios (δ), minimum value of χ^2 fit, and corresponding spin-parity combination of initial and final state for the observed γ transitions in ^{108}In .

E_γ (keV)	I_γ	A_{22}	A_{44}	δ	χ^2_{red}	$J_i^\pi \rightarrow J_f^\pi$
147.1	29.1	-0.24(2)	-0.03(2)	0.02(3)	1.5	$10^- \rightarrow 9^-$
				-0.09(3)	1.6	$8^- \rightarrow 9^-$
154.0	38.3	-0.25(2)	-0.01(2)	0.02(3)	1.6	$11^- \rightarrow 10^-$
				-0.08(3)	1.9	$9^- \rightarrow 10^-$
213.6	70.9	-0.26(1)	0.01(1)	0.04(4)	0.7	$8^- \rightarrow 7^-$
				-0.12(4)	1.4	$6^- \rightarrow 7^-$
223.7	5.3	-0.23(3)	0.04(3)	-0.01(3)	0.7	$10^- \rightarrow 9^-$
				-0.05(3)	0.6	$8^- \rightarrow 9^-$
231.4	45.5	-0.27(1)	0.02(1)	0.02(2)	2.0	$12^- \rightarrow 11^-$
				-0.06(2)	2.9	$10^- \rightarrow 11^-$
256.9	5 ^b	^a				
294.6	1.2	-0.41(6)	0.16(5)	0.19(6)	4.3	$14^- \rightarrow 13^-$
				-0.08(8)	4.8	$12^- \rightarrow 13^-$
322.6	5.0	-0.25(3)	0.05(3)	0.00(2)	0.9	$11^- \rightarrow 10^-$
				-0.05(2)	0.9	$9^- \rightarrow 10^-$
336.1	33.8	-0.28(2)	0.05(2)	0.01(2)	3.4	$13^- \rightarrow 12^-$
				-0.06(2)	3.3	$11^- \rightarrow 12^-$
349.8	14.1	-0.10(2)	-0.01(2)	-0.08(3)	0.4	$11^- \rightarrow 10^-$
				0.04(3)	0.4	$9^- \rightarrow 10^-$
357.9	9.5	-0.27(3)	0.04(4)	0.01(4)	1.8	$13^- \rightarrow 12^-$
				-0.06(4)	1.8	$11^- \rightarrow 12^-$
413.9	4.1 ^b	^a				
473.6	9.3	-0.19(3)	-0.01(3)	0.06(4)	0.2	$14^- \rightarrow 13^-$
				-0.01(5)	0.2	$12^- \rightarrow 13^-$
527.2	26.0			-0.06(4)	2.6	$9^- \rightarrow 8^-$
529.2	30.8	-0.15(2) ^c	0.05(2)	0.01(4)	2.5	$7^- \rightarrow 8^-$
542.5	13.1	-0.26(3)	-0.05(4)	0.04(3)	0.7	$11^- \rightarrow 10^-$
				-0.10(4)	0.8	$9^- \rightarrow 10^-$
				1.4(3)	4.5	$10^- \rightarrow 10^-$
565.3	8.9	-0.08(3)	0.08(3)	-0.10(6)	1.9	$15^- \rightarrow 14^-$
				0.09(5)	1.9	$13^- \rightarrow 14^-$
585.5	6.4 ^b	^a				
604.8	27.5	-0.22(2)	0.07(2)	-0.02(4)	4.2	$10^- \rightarrow 9^-$
				-0.03(5)	4.1	$8^- \rightarrow 9^-$
661.7	17.6	-0.10(3)	-0.08(4)	-0.01(4)	2.9	$15^- \rightarrow 14^-$
				0.03(5)	2.9	$13^- \rightarrow 14^-$
				0.9(2)	4.6	$14^- \rightarrow 14^-$

TABLE II. (Continued).

E_γ (keV)	I_γ	A_{22}	A_{44}	δ	χ^2_{red}	$J_i^\pi \rightarrow J_f^\pi$
1119.7	100	-0.29(2)	0.05(2)	0.02(3)	3.4	$7^- \rightarrow 6^+$
				-0.13(5)	3.4	$5^- \rightarrow 6^+$
1182.7	21.4	0.38(3)	-0.08(3)	-0.43(10)	4.9	$9^- \rightarrow 8^-$
				-0.05(6)	1.9	$10^- \rightarrow 8^-$
				-0.47(19)	2.0	$8^- \rightarrow 8^-$
				0.57(18)	4.1	$7^- \rightarrow 8^-$
				0.28(8)	4.2	$6^- \rightarrow 8^-$
1329.9	15.5	0.38(4)	-0.16(4)	-0.02(3)	3.8	$10^- \rightarrow 8^-$
				-0.56(11)	4.3	$8^- \rightarrow 8^-$
1396.3	15.8 ^b	0.30(2) ^c	-0.10(2)	0.02(3)	1.8	$9^- \rightarrow 7^-$
				-0.7(2)	4.3	$7^- \rightarrow 7^-$

^aAngular distribution could not be analyzed due to strong admixture (see text).

^bIntensity deduced from coincidence intensities.

^cCoefficients given for unresolved doublet.

to the 393 and 414 keV transitions from lines in ^{105}Cd and ^{108}In , respectively.

B. ^{108}In

In Fig. 9 the proposed level scheme for ^{108}In is shown. The high-spin isomer (58 min) state of ^{108}In

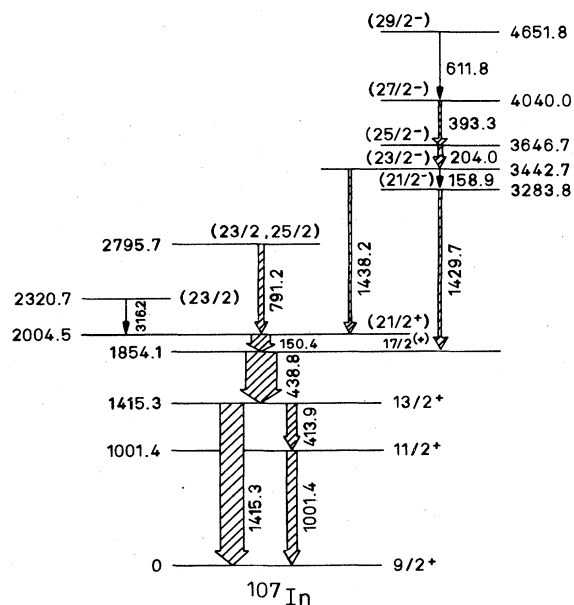


FIG. 7. Level scheme proposed for ^{107}In . The widths of the arrows are proportional to the decay intensities in the $^{92}\text{Mo}(^{19}\text{F}, 2p 2n \gamma)^{107}\text{In}$ reaction at 70 MeV.

has been assigned $I^\pi = 6^+$ from a β^+/EC decay study,³¹ but also $I^\pi = 7^+$ has been suggested for this state from linear polarization measurements.³² In this work the level scheme is based on the 6^+ assignment of the ground state. The assignment of the 1120 keV line feeding the ground state as an $E1$ transition is in agreement with the linear polarization data of Ref. 14. From the level scheme and the spins established by the lines $E_\gamma = 214$, 1330, 1396, and 147 keV it follows (see Table II) that the 1183 keV line is a strongly mixed ($\delta \cong -0.43$) $M1/E2$ transition. This conclusion is

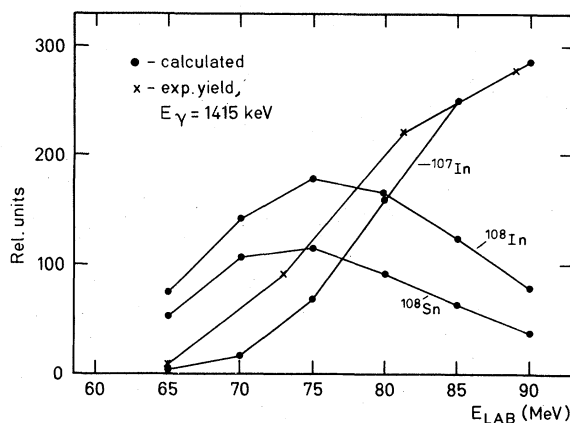


FIG. 8. Statistical model calculations of the total yields of residual nuclei in the reaction $^{92}\text{Mo}(^{19}\text{F}, xyz)$ as a function of bombarding energy compared to the experimental yield of the 1415 keV line in ^{107}In . The experimental yield was normalized to the calculated value for ^{107}In at 89 MeV. Only the calculated curves for the three strongest populated residual nuclei are shown.

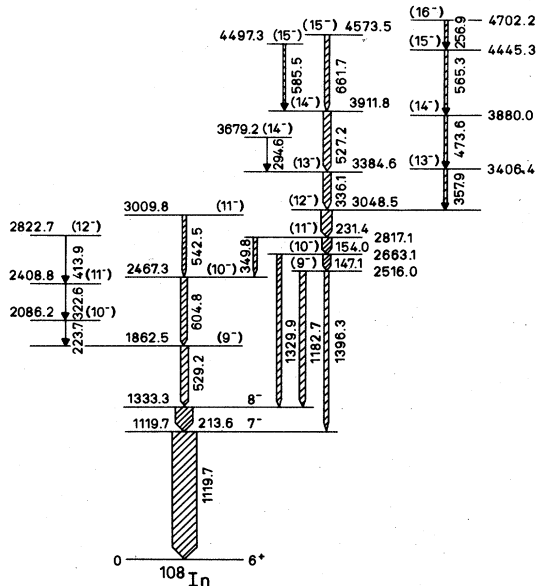


FIG. 9. Level scheme proposed for ^{108}In . The widths of the arrows are proportional to the decay intensities in the $^{92}\text{Mo}(^{19}\text{F}, 2pn\gamma)^{108}\text{In}$ reaction at 70 MeV.

supported by the linear polarization results of Ref. 14. Except for the two $E2$ transitions 1330 and 1396 keV, all other lines observed are found to have angular distributions consistent with $M1$ multipolarity, i.e., all states found above the 7^- level at 1119.7 keV have negative parity.

For the 257, 414, and 585 keV transitions no reliable angular distribution information could be obtained, as these lines were strongly admixed by transitions in ^{108}Sn , ^{107}In , and ^{108}Sn , respectively. This made the placement of the 257 keV line somewhat uncertain; however, it clearly belongs to the band with the 358, 474, and 565 keV lines. As the majority of the lines observed has $M1$ character, an $M1$ multipolarity was assumed for the 257, 414, and 585 keV transitions in the proposed level scheme.

IV. DISCUSSION

A. ^{107}In

For the first two excited states in ^{107}In observed in this work, we propose, because of the selectivity of the reaction for high spins, the highest of the spin values suggested by Dietrich *et al.*⁵ ($I^\pi = \frac{11}{2}^+$ and $\frac{13}{2}^+$, respectively). All the higher lying levels are introduced here for the first time.

The level characteristics of high-spin states in ^{109}In and ^{111}In have been interpreted within a

hole-core coupling model.^{12,13} Figure 10 shows a comparison of the observed positive-parity states in ^{107}In with the corresponding states in ^{108}Sn .²⁴ Calculations made for the one-phonon multiplet with the hole-core coupling model have shown fairly good agreement with experimental results for the $^{109,111}\text{In}$ (Refs. 12,13) and $^{113,115}\text{In}$ (Refs. 10,11) isotopes. The coupling of a $g_{9/2}$ proton hole to a one-phonon excitation of the ^{108}Sn core may also adequately describe the situation in ^{107}In as can be seen in Fig. 10. The theoretical predictions for a two-phonon multiplet in ^{111}In (Ref. 13) were in poorer agreement with experiment. This disagreement was assumed¹³ to be due to the nature of the 4_1^+ state in ^{112}Sn which cannot be considered as a pure two-phonon state, but is more likely a two-quasiparticle state, as this is the case also for the 6_1^+ state. So, the $\frac{21}{2}^+$ state in ^{111}In was suggested to be a hole-two-quasiparticle state.¹³ Similarly, a reasonable explanation of the $\frac{17}{2}^+$ and $\frac{21}{2}^+$ states in ^{107}In within a hole-core coupling picture is the coupling of a $g_{9/2}$ proton hole to the excited two-quasineutron ^{108}Sn core states with $I^\pi = 4^+$ and 6^+ , respectively (cf. Fig. 10). The dominant configurations of these two-quasiparticle core states should be $(\nu d_{5/2})^2$, $(\nu g_{7/2})^2$, and $(\nu d_{5/2})(\nu g_{7/2})$.

The sequence of positive parity states in ^{107}In shows resemblances to that in ^{111}In .¹³ However, no $\frac{15}{2}^+$ state has been found in ^{107}In , and another difference is the considerable lowering in excitation energy ($\cong 700$ keV) of the $\frac{17}{2}^+$ and $\frac{21}{2}^+$ states in ^{107}In compared to ^{111}In . The properties of the positive-parity states in ^{109}In as observed in Ref. 12 are somewhat different. There, surprisingly, no

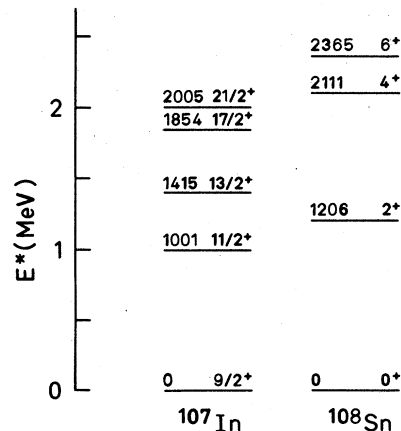


FIG. 10. Positive-parity states in ^{107}In compared with corresponding states in ^{108}Sn (see text).

$\frac{21}{2}^+$ state has been identified. Furthermore, a long-living ($T_{1/2} = 0.21$ s) $I^\pi = \frac{19}{2}^+$ isomeric state decaying via an $M3$ transition was observed,¹² which these authors could not explain within the hole-core coupling model.

In Fig. 11 the negative-parity states identified in ^{107}In are compared to the corresponding core states in ^{108}Sn .²⁴ One can see also that for the negative-parity states in ^{107}In a hole-core coupling picture could qualitatively account for the level sequence.

The "rotational-like" band structure of the negative-parity high-spin states in ^{107}In connected by $\Delta I = 1$ transitions can also be seen in $^{109,111}\text{In}$.^{12,13} As the even Cd isotopes can be well described within a rotational model^{8,9} one could think of explaining the features of the negative-parity states in ^{107}In by a one-quasiparticle + slightly deformed rotor model. However, neither in ^{107}In nor in $^{109,111}\text{In}$ (Refs. 12,13) have $\Delta I = 2$, $E2$ transitions between the band members been observed.

B. ^{108}In

The level scheme for ^{108}In as proposed by Elias *et al.*¹⁴ is extended by many new high-spin states. The main part of the level scheme of Ref. 14 is confirmed; however, their "extra" cascade formed by the 237 and 1396 keV transitions we have preferred not to assign to ^{108}In . In Ref. 14 this assignment was made only on the basis of excitation function measurements. In this case this is a rather dubious procedure, as at least the 1396 keV line is strongly admixed. Also, the relative excitation function of the 237 keV line does not convincingly look as if the transition deexcites a high-spin state in ^{108}In .

The dominance of $\Delta I = 1$ transitions in the level scheme is striking. Similar to the situation in ^{107}In , rotational-like bands occur with only a few inter-band transitions. This may lead to an interpretation with a two-quasiparticle + slightly deformed rotor model. Calculations with such a model have been carried out in Ref. 14 and the results fairly well

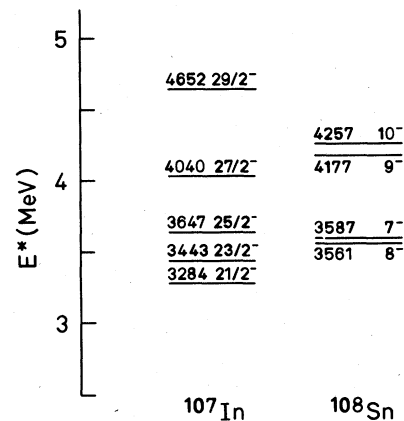


FIG. 11. Negative-parity states in ^{107}In compared with corresponding states in ^{108}Sn (see text).

reproduce the lower band built on the 7^- state at 1333 keV. A similar model has been found appropriate to describe the features of the odd-odd $^{196,198}\text{Tl}$ nuclei^{33,34} which also have one proton hole in a closed shell ($Z = 81$).

In Refs. 33 and 34 the model of the odd-odd Tl nuclei was a deformed Hg core plus two quasiparticles. Thereby each level of the ground state band in the core nucleus would give rise to two yrast states with a difference of one spin unit, thus leading to a $\Delta I = 1$ band in the Tl spectrum. ^{106}Cd , which is known to show rotor properties,⁹ would be the corresponding core for ^{108}In .

As the energy gap between the band heads of the two dominating bands corresponding to the 1396 keV transition is comparable to the excitation energy of the 2_1^+ state in ^{110}Sn (1212 keV), another possible interpretation, as suggested in Ref. 14, is that these band heads are built up by a $(\pi g_{9/2})^{-1} \times (\nu h_{11/2})^{-1}$ configuration coupled to the 0^+ and the one-phonon 2^+ states of the ^{110}Sn core, respectively.

It is a pleasure for the authors to thank Dr. R. Männer for his effective help in setting up programs for the PDP 11/45 computer.

*On leave from Institute of Nuclear Research of the Ukrainian Academy of Science, Kiev, USSR.

¹M. Conjeaud, S. Harar, and E. Thuriere, Nucl. Phys. **A129**, 10 (1969).

²C. V. Weiffenbach and R. Tickle, Phys. Rev. **C 3**, 1668

(1971).

³A. van Poelgeest, J. Bron, W.H.A. Hesselink, K. Allaart, J.J.A. Zalmstra, M. J. Uitzinger, and H. Verheul, Nucl. Phys. **A346**, 70 (1980).

⁴J. McDonald, B. Fogelberg, A. Bäcklin, and Y. Kawase,

- Nucl. Phys. A224, 13 (1974).
- ⁵W. Dietrich, A. Bäcklin, C. O. Lannergård, and I. Ragnarsson, Nucl. Phys. A253, 429 (1975).
- ⁶J. Bron, W.H.A. Hesselink, A. van Poelgeest, J.J.A. Zalmstra, M. J. Uitzinger, and H. Verheul, Nucl. Phys. A318, 335 (1979).
- ⁷B. Nerlo-Pomorska and J. Ludziejewski, Z. Phys. A 287, 337 (1978).
- ⁸L. E. Samuelson, F. A. Rickey, J. A. Grau, S. I. Popik, and P. C. Simms, Nucl. Phys. A301, 159 (1978).
- ⁹L. E. Samuelson, J. A. Grau, S. I. Popik, F. A. Rickey, and P. C. Simms, Phys. Rev. C 19, 73 (1979).
- ¹⁰F. S. Dietrich, B. Herskind, R. A. Naumann, R. G. Stokstad, and G. E. Walker, Nucl. Phys. A155, 209 (1970).
- ¹¹W. K. Tuttle, P. H. Stelson, R. L. Robinson, W. T. Milner, F. K. McGowan, S. Roman, and W. K. Dagenhart, Phys. Rev. C 13, 1036 (1976).
- ¹²A. van Poelgeest, W.H.A. Hesselink, J. Bron, J.J.A. Zalmstra, M. J. Uitzinger, H. Verheul, S. J. Feenstra, and J. van Klinken, Nucl. Phys. A327, 12 (1979).
- ¹³W.H.A. Hesselink, J. Bron, P.M.A. van der Kam, V. Paar, A. van Poelgeest, and A. G. Zephat, Nucl. Phys. A299, 60 (1978).
- ¹⁴N. Elias, R. Béraud, A. Charvet, R. Duffait, M. Meyer, S. André, J. Genevey, S. Tedesco, J. Tréherne, F. Beck, and T. Byrski, Nucl. Phys. A351, 142 (1981).
- ¹⁵M. Eibert, A. K. Gaigalas, and N. I. Greenberg, J. Phys. G 2, L203 (1976).
- ¹⁶G. Poggel, A. Faessler, and K. W. Schmid, Z. Phys. A 299, 55 (1981).
- ¹⁷H. V. Klapdor, in *Lecture Notes in Physics, Vol. 92* (Springer, Berlin, 1979), pp. 125–139.
- ¹⁸M. Schrader, A. Szanto, and H. V. Klapdor, Z. Phys. A 289, 193 (1979).
- ¹⁹E. M. Szanto, A. Szanto, H. V. Klapdor, M. Diebel, J. Fleckner, and U. Mosel, Phys. Rev. Lett. 42, 622 (1979).
- ²⁰H. V. Klapdor, Nukleonika 25, 289 (1980).
- ²¹P. Baumann, A. M. Bergdolt, G. Bergdolt, A. Huck, G. Walter, H. V. Klapdor, H. Fromm, and H. Willmes, Phys. Rev. C 18, 247; 18, 2110 (1978).
- ²²P. Kofahl-Herges, H. Fromm, H. V. Klapdor, and T. Oda, Proceedings of the International Conference on Nuclear Physics, Berkeley, 1980 (LBL Report No. LBL-11118), p. 367.
- ²³H. Fromm, H. V. Klapdor, and P. Herges J. Phys. G 7, L109 (1981).
- ²⁴E. Andersson, P. Herges, H. V. Klapdor, and I. N. Wischnewski, Z. Phys. A 299, 105 (1981).
- ²⁵I. N. Wischnewski, H. V. Klapdor, H. Fromm, and P. Herges, Z. Phys. A 301, 29 (1981).
- ²⁶I. N. Wischnewski, H. V. Klapdor, P. Herges, H. Fromm, and W. A. Zheldonozhski, Z. Phys. A 298, 21 (1980).
- ²⁷P. Kofahl-Herges and H. V. Klapdor, Max-Planck-Institut, Heidelberg, Annual Report (1978), p. 24; P. Herges, Ph.D. thesis, Ruprecht-Karls-Universität, 1980.
- ²⁸F. Pühlhofer, Nucl. Phys. A280, 267 (1977).
- ²⁹T. Yamazaki and G. T. Ewan, Nucl. Phys. A134, 81 (1969).
- ³⁰E. Thuriere, Ph.D. thesis, University of Grenoble, 1969.
- ³¹S. Flanagan, R. Chapman, G. D. Dracoulis, J. L. Durell, W. Gelletly, A. J. Hartley, and J. N. Mo, J. Phys. G 1, 77 (1975).
- ³²D. C. Stromswold, D. O. Elliott, Y. K. Lee, L. E. Samuelson, J. A. Grau, F. A. Rickey, and P. C. Simms, Phys. Rev. C 17, 143 (1978).
- ³³A. J. Kreiner, M. Fenzl, and W. Kutschera, Nucl. Phys. A308, 147 (1978).
- ³⁴A. J. Kreiner, M. Fenzl, S. Lunardi, and M.A.J. Mariscotti, Nucl. Phys. A282, 243 (1977).